Enhanced luminescence from Tb for the mixed spinel $Mg_xZn_{1-x}Al_2O_4$

W A I Tabaza, H C Swart and R E Kroon

Department of Physics, University of the Free State, IB51, P. O. Box 339, Bloemfontein, 9300, South Africa

E-mail: KroonRE@ufs.ac.za

Abstract. $MgAl_2O_4$ and $ZnAl_2O_4$ are ceramics of the spinel structure which, amongst diverse applications, have been used as phosphor hosts activated by a variety of transition metal and lanthanide ions. Both have been studied separately as possible hosts for Tb^{3+} ions, but in this work they are compared directly. Results were also obtained for the mixed spinels $Mg_xZn_{1-x}Al_2O_4$, which are of interest because although the lattice constant changes very little with composition, the bandgap of $MgAl_2O_4$ (7.8 eV) is double that of $ZnAl_2O_4$ (3.9 eV). Nanocrystalline powder samples with a particle size of about 25 nm were prepared using the combustion method. For $MgAl_2O_4$:Tb(0.5 mol%) both green emissions due to $^5D_4$-^7F_J transitions (with the most intense $^5D_4$-$^7F_5$ transition at 544 nm) and blue emissions due to $^5D_3$-^7F_J transitions were observed. Less intense green emissions were observed for $ZnAl_2O_4$:Tb(0.5 mol%) and no blue emission occurred. Both samples had similar excitation spectra (for the 544 nm emission), with a peak near 230 nm which is attributed to the Tb 4f-5d transition. This was unexpected, considering to the large difference in their bandgaps. This excitation wavelength corresponds to an energy of 5.4 eV which is higher than the bandgap of $ZnAl_2O_4$. Therefore a fraction of the incident light will be absorbed by this host and not be available to excite the Tb ions, which corresponds to the observation of poorer luminescence from the $ZnAl_2O_4$:Tb. The absence of blue emission peaks is usually attributed to concentration quenching, but since the same Tb concentration was used for the $MgAl_2O_4$:Tb where blue emissions did occur, it is rather suggested that because of the smaller bandgap of $ZnAl_2O_4$, the $^5D_3$ level lies close to or inside the conduction band and this prevents transitions from this level. The maximum green emission was measured for $Mg_{0.75}Zn_{0.25}Al_2O_4$:Tb(0.5 mol%), although the blue emissions from this sample were less than for the $MgAl_2O_4$ host.

1. Introduction

Spinels, which have the general formula AB_2O_4, often occur naturally as minerals but are also synthesized and studied for their interesting electrical, magnetic and optical properties. $MgAl_2O_4$ finds diverse applications due to its mechanical strength, chemical inertness, relatively low density, high melting point, high thermal shock resistance, low thermal expansion coefficient, resistance to neutron irradiation and low dielectric loss, and has been used for humidity sensors [1] and tuneable solid-state lasers [2]. $ZnAl_2O_4$ is widely used as a catalyst and has also been patented for UV reflective optical coatings [3]. It is electroconductive and has been considered for thin film electroluminescent and plasma displays, as well as for ultraviolet (UV) photo-electronic devices and stress sensors [4-6]. Both materials have been used as phosphor hosts for a variety of luminescent ions [7,8] and $MgAl_2O_4$:Mn

has used as green phosphor for television tubes [9] while $MgAl_2O_4$:Ce has been investigated as a long afterglow phosphor [10]. An important difference between the materials is that the bandgap of $MgAl_2O_4$ (7.8 eV [11]) is much larger than that of $ZnAl_2O_4$ (3.8-4.1 eV [12]). However, since Mg and Zn ions are similar in size, the lattice constants of these materials are close to one another and it is interesting to consider the intermediate material $Mg_xZn_{1-x}Al_2O_4$ as a possible phosphor host. In this paper, the combustion method is used to prepare undoped as well as Tb^{3+}-doped $Mg_xZn_{1-x}Al_2O_4$ with different proportions of Mg ($0 \leq x \leq 1$), and the structural and optical properties are reported.

2. Experimental

$Mg_xZn_{1-x}Al_2O_4$ was prepared using the combustion method according to the reaction

$$3Mg(NO_3)_2[x] + 3Zn(NO_3)_2[1-x] + 6Al(NO_3)_3 + 20\ CH_4N_2O \rightarrow 3Mg_xZn_{1-x}Al_2O_4 + 32N_2 + 20CO_2 + 40H_2O$$

where the waters of crystallization of the nitrates have been omitted for simplicity. Analytical grade $Al(NO_3)_3{\cdot}9H_2O$, $Zn(NO_3)_2{\cdot}4H_2O$ and $Mg(NO_3)_2{\cdot}6H_2O$ were used as oxidizers and urea (CH_4N_2O) was used as a fuel. Generally about 10 mmol of $Al(NO_3)_3.9H_2O$ was added to stoichiometric amounts of the other reactants in about 6 ml of distilled water, which was stirred vigorously for 30 min to obtain a homogeneous transparent solution. In some cases MgO dissolved in concentrated nitric acid was used as the source of magnesium nitrate. The solution was transferred to a porcelain crucible and placed into a muffle furnace at 520°C. Within a few minutes the water boiled off and the sample ignited as the exothermic combustion reaction occurred, giving off copious quantities of gas and heating the material to well above the furnace temperature. After the reaction the foamy white product was removed from the furnace and crushed into powder using a pestle and mortar, after which it was annealed in air at 700°C for 4 hours. Doping of samples with Tb^{3+} ions was achieved by replacing an appropriate amount of $Al(NO_3)_3{\cdot}9H_2O$ with the same amount of $Tb(NO_3)_3.5H_2O$.

X-ray diffraction (XRD) measurements were made at room temperature using a Bruker D8 Advance diffractometer operating at 40 kV and 40 mA with Cu Kα x-rays of wavelength 154.178 pm. A Shimadzu SSX-550 scanning electron microscope (SEM) was used to obtain images of the samples. Luminescence properties were measured at room temperature using a Cary Eclipse fluorescence spectrophotometer and excitation spectra were measured at 10 K using synchrotron radiation at the SUPERLUMI station at DESY [13] and corrected for the response of the system using sodium salicylate.

3. Results and discussion

3.1. Structure

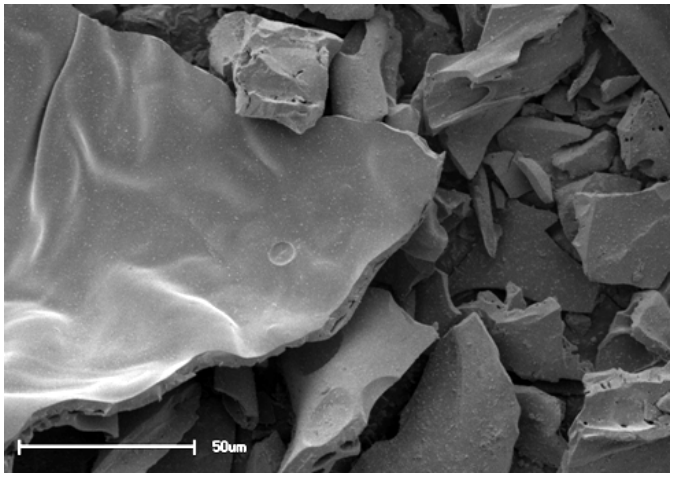

Figure 1. SEM image of $Mg_{0.75}Zn_{0.25}Al_2O_4$:Tb 0.5 mol% produced with the combustion method.

Figure 1 shows a SEM image of one of the samples ($Mg_{0.75}Zn_{0.25}Al_2O_4$:Tb 0.5 mol%) after the combustion process. It reveals the formation of different sized agglomerates displaying an irregular morphology in the form of plates. The pores are consistent with the fact that a large amount of gas evolves during the combustion synthesis.

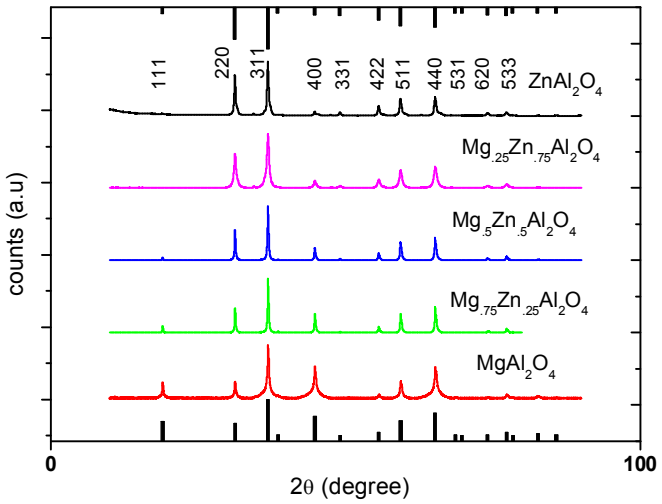

Figure 2. X-ray diffraction spectra of $Mg_xZn_{1-x}Al_2O_4$.

The XRD spectra of undoped $Mg_xZn_{1-x}Al_2O_4$ before and after annealing revealed no significant differences and the results from the annealed samples are shown in figure 2, together with the expected patterns for $MgAl_2O_4$ (JCPDS 75-0710) and $ZnAl_2O_4$ (JCPDS 82-1043) spinels. These correspond very well to the experimental results, confirming the successful preparation of the host materials. From the positions of the peaks it is clear that the lattice parameter changes very little between the two materials and that $Mg_xZn_{1-x}Al_2O_4$ has the same spinel structure irrespective of the magne sium content (x). This is due to the similar ionic radii of Mg^{2+} (58.5 pm) and Zn^{2+} (58 pm) [14]. However, the x-ray scattering factor of Zn is greater than that of Mg due to its higher atomic number (more electrons) and so the relative size of the x-ray diffraction peaks vary significantly with composition, as can be seen by comparing the heights of the (220) and (400) reflections relative to the (311) reflection between them.

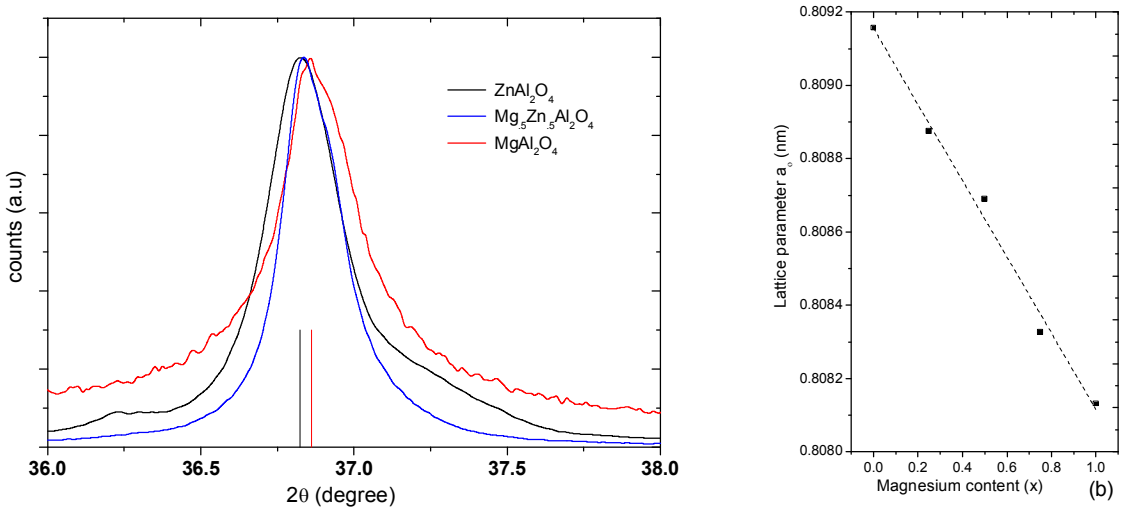

Figure 3. (a) Detail of (311) XRD peak of $Mg_xZn_{1-x}Al_2O_4$. (b) Lattice parameter of $Mg_xZn_{1-x}Al_2O_4$ as a function of composition. The line is a least squares fit to the data.

Figure 3(a) shows the (311) XRD reflection in more detail, together with the expected 2θ position in $MgAl_2O_4$ and $ZnAl_2O_4$. Figure 3(b) shows the lattice parameter as a function of composition and it varies linearly between the values for the boundary compounds. The width of this peak does not vary substantially with composition and its full-width-at-half-maximum was used to determine the crystallite size of about 25 nm using the Scherrer equation $D = 0.9\lambda/(\beta \cos\theta)$, where λ is the x-ray wavelength and θ the diffraction angle. In figure 3(a) small peak on the low angle side can be seen for $ZnAl_2O_4$ (at 36.2°) which is absent for $MgAl_2O_4$. This peak is due to a small amount of ZnO impurity formed during the reaction, and could not easily be removed by varying the quantities of reactants during the combustion process. No extra peaks were observed in the samples doped with Tb^{3+}, indicating that it was successfully incorporated in the lattice, where it is assumed that it substitutes the Al^{3+} ions which have the same valency [15].

3.2. Optical properties

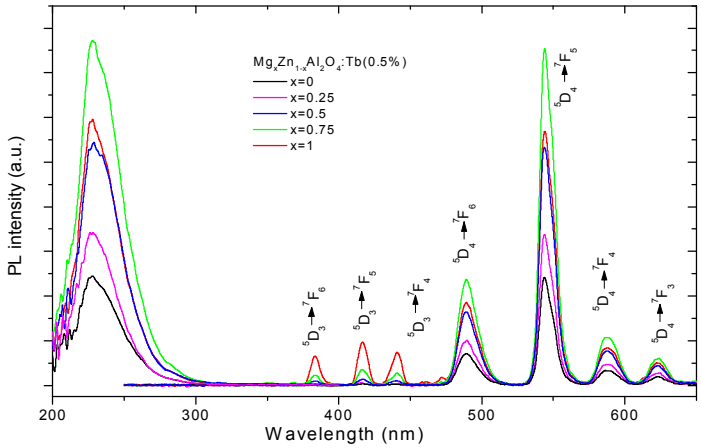

Figure 4. Room temperature excitation and emission spectra of $Mg_xZn_{1-x}Al_2O_4$ measured with the Cary Eclipse.

Figure 4 shows the photoluminescence excitation and emission spectra for the $Mg_xZn_{1-x}Al_2O_4$:Tb(0.5 mol%) samples measured with the Cary-Eclipse. Together with usual green emission from Tb^{3+} ions in the wavelength region longer than 480 nm, corresponding to $^5D_4 \rightarrow {}^7F_J$ (J=3,4,5,6) transitions, there is also blue emission below 480 nm corresponding to $^5D_3 \rightarrow {}^7F_J$ (J=4,5,6) transitions for some samples. As is common for hosts doped with Tb, the green $^5D_4 \rightarrow {}^7F_5$ emission line at 544 nm is the strongest.

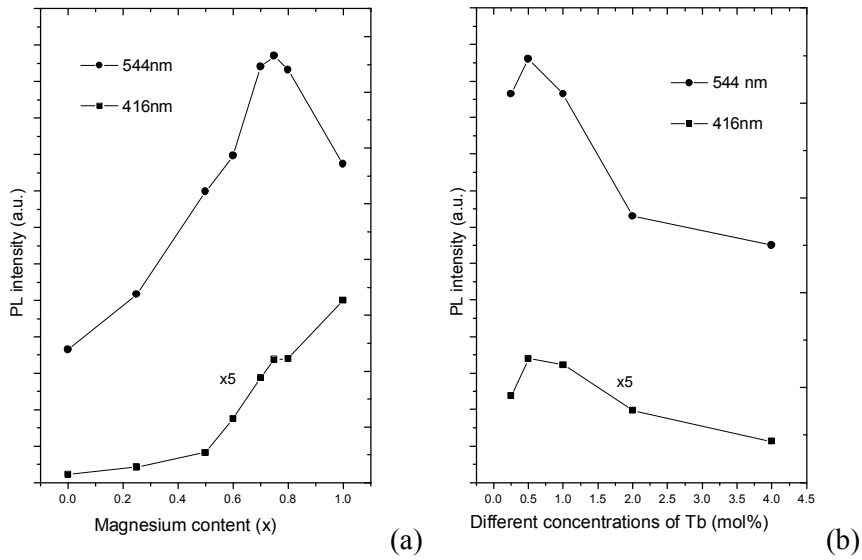

Figure 5.
Intensity of the green (544 nm) and blue (416 nm) luminescence from:
(a) $Mg_xZn_{1-x}Al_2O_4$:Tb(0.5 mol%) as a function of composition.
(b) $Mg_{0.75}Zn_{0.25}Al_2O_4$:Tb for different Tb doping concentrations.

Figure 5(a) shows the intensity of the green (544 nm) and blue (416 nm) luminescence as a function of composition. The intensity of the blue emission from the $^5D_3$ level increases with increasing Mg concentration. The relative intensity of the blue and green emissions from Tb are often discussed in terms of cross-relaxation effects [16], where for low concentrations of Tb^{3+} ions which are then isolated from one another blue emission from the $^5D_3$ level can be observed, whereas when the Tb concentration is increased, electrons excited to the $^5D_3$ level may transfer some of their energy to neighbouring Tb^{3+} ions and thereby drop to the $^5D_4$ level, from which they emit radiatively instead of from the $^5D_3$ level. However, since all the samples in figure 5(a) are doped to the same Tb concentration of 0.5 mol%, this cross-relaxation effect cannot simply explain the observed change in the blue emission. If clustering of Tb ions occurs more predominantly in the samples containing small amounts of Mg then cross-relaxation may indeed play a role, but a more likely explanation of the effect is the changing size of the bandgap as a function of composition. $ZnAl_2O_4$ has the smallest bandgap and therefore the Tb $^5D_3$ level will lie closest (or possibly inside) the conduction band for this material. Electrons excited to the $^5D_3$ level could therefore be transferred to the conduction band, which would account for the lack of blue emissions from this level. With increasing Mg content the bandgap increases and blue emission from the $^5D_3$ level becomes possible, and increases in intensity as the level moves further from the conduction band. The maximum green emission occurs for the intermediate composition $Mg_{0.75}Zn_{0.25}Al_2O_4$ and is superior to that of both $ZnAl_2O_4$ and $MgAl_2O_4$. Figure 5(b) shows the Tb emission intensity as a function of doping concentration for this composition. The maximum intensity occurs for the Tb^{3+} concentration of 0.5 mol%, in agreement with the value reported previously for $MgAl_2O_4$:Tb [17].

The Tb^{3+} excitation spectra in figure 4 (measured with the Cary-Eclipse using the green $^5D_4 \rightarrow {}^7F_5$ emission line at 544 nm) consist of broad bands in the region from 220 to 300 nm originating from the f-d transition. A small shift in the peak with changing composition is apparent. Although the relative intensity of these peaks is reliable, the spectra are not corrected for the response of the system, which can only measure down to 200 nm since this is the range of the xenon lamp. Low temperature (10 K) excitation spectra extending down to 100 nm and corrected for the system response were measured for the same transition using synchrotron radiation at SUPERLUMI (DESY) and are shown in figure 6. Here the relative intensities are not reliable due to the increased challenge of positioning samples reproducibly, but the excitation curve is accurate.

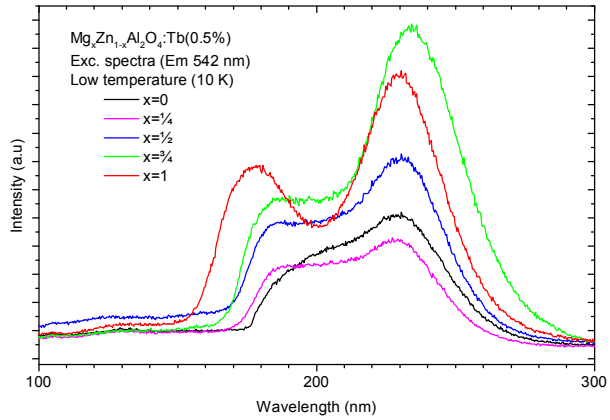

Figure 6. Low temperature excitation spectra of $Mg_xZn_{1-x}Al_2O_4$ measured at SUPERLUMI.

From figure 6 it is clear that the excitation bands measured with the Cary-Eclipse (figure 4) are truncated at shorter wavelengths and that more than one excitation band occurs. Generally there are five allowed f-d transitions for Tb [18], which have been modelled in several hosts [19]. In $Y_3(Al_{1-x}Ga_x)_5O_{12}$ the peak positions have been found to shift apart as the Ga content decreases and the bandgap increases [20]. Although five distinct bands cannot be identified in our spectra, the range of the f-d excitation region is not dissimilar to that reported for Tb in other hosts and a widening of the

region with increasing Mg content and therefore bandgap is apparent. On the short wavelength side there is a shift to shorter wavelengths as the Mg content increases, but on the longer wavelength side the extreme excitation spectrum corresponds to x = 0.75, which also corresponds to the maximum green emission intensity. The wavelength corresponding to the host bandgap energy varies from about 130 nm for $MgAl_2O_4$ to 260 nm for $ZnAl_2O_4$, and although the f-d excitation overlaps most of this region, it does not appear that there is an excitation peak corresponding to band-to-band transitions i.e. the Tb is not excited through the host.

4. Conclusion

The mixed spinel $Mg_xZn_{1-x}Al_2O_4$ has been successfully synthesized using the combustion method and doped with Tb. The maximum PL intensity of the green emission at 544 nm occurred for $Mg_{0.75}Zn_{0.25}Al_2O_4$ and the optimum Tb concentration was found to be 0.5 mol%. The blue emission at 416 nm was almost absent for $ZnAl_2O_4$, but increased with the Mg content and was a maximum for $MgAl_2O_4$. This is attributed to the increasing bandgap with Mg content.

Acknowledgments

The National Research Foundation is acknowledged for financial assistance. The authors thank H Grobler at the University of the Free State Centre for Microscopy for assisting with the SEM measurements, and A Kotlov at DESY for assistance with synchrotron measurements.

References

[1] Shpotyuk O, Ingram A, Klym H, Vakiv M, Hadzaman I and Filipecki J 2005 *J. Eur. Ceram. Soc.* **25** 2981
[2] Jouini A, Yoshikawa A, Guyot Y, Brenier A, Fukuda T and Boulon G 2007 *Opt. Mat.* **30** 47
[3] Cordaro, JF. 1998 US Patent No. 5820669
[4] García-Hipólito M, Hernández-Pérez CD, Alvarez-Fregoso O, Martínez E, Guzmán-Mendoza J and Falcony C 2003 *Opt. Mat.* **22** 345
[5] Lou Z and Hao J 2004 *Thin Solid Films* **450** 334
[6] Lou Z and Hao J 2005 *Appl. Phys. A* **80** 151
[7] Tshabalala KG, Cho S-H, Park J-K, Pitale SS, Nagpure IM, Kroon RE, Swart HC and Ntwaeaborwa OM 2011 *J. Alloys Compds* **509** 10115
[8] Wiglusz RJ and Grzyb T 2011 *Opt. Mat.* **33** 1506
[9] Maiman, TH, Hoskins, RH, Soffer, BH, Pastor, RC and Pearson, MA. 1968 US Patent No. 3396119
[10] Jia D and Yen WM 2003 *J. Lumin.* **101** 115
[11] Sampath SK, Kanhere DG and Pandey R 1999 *J. Phys.: Condens. Matter* **11** 3635
[12] Dixit H, Tandon N, Cottenier S, Saniz R, Lamoen D, Partoens B, van Speybroeck V and Waroquier M 2011 *New J. Phys.* **13** 063002
[13] Zimmerer G 2007 *Rad. Meas.* **42** 859
[14] O'Neil, HS-C and Navrotsky, A 1983 *American Minerologist* **68** 181
[15] Silva D, Abreu A, Davolos MR and Rosaly M 2011 *Opt. Mat.* **33** 1226
[16] Park JY, Jung HC, Raju GSR, Moon BK, Jeong JH, Kim JH 2010 *J. Lumin.* **130** 478
[17] Aluga Raja E, Dhabekar B, Menon S, More SP, Gundu Rao TK and Kher RK 2009 *Indian J. Pure & Applied Phys.* **47** 420
[18] Dorenbos P 2003 *J. Phys.: Condens. Matter* **15** 6249
[19] van Pieterson L, Reid MF, Burdick GW and Meijerink A 2002 *Phys Rev B* **65** 045114
[20] Mayolet A, Zhang W, Simoni E, Krupa JC and Martin P 1995 *Opt. Mat.* **4** 757